ACS Infectious Diseases

pubs.acs.org/journal/aidcbc
Article

Heterologous Sarbecovirus Receptor Binding Domains as Scaffolds for SARS-CoV-2 Receptor Binding Motif Presentation

Blake M. Hauser, Maya Sangesland, Evan C. Lam, Kerri J. St Denis, Maegan L. Sheehan, Mya L. Vu, Agnes H. Cheng, Sophia Sordilla, Dana Thornlow Lamson, Ahmad W. Almawi, Alejandro B. Balazs, Daniel Lingwood, and Aaron G. Schmidt*

Cite This: ACS Infect. Dis. 2024, 10, 553−561

Read Online

ACCESS | Metrics & More | Article Recommendations | Supporting Information

ABSTRACT: Structure-guided rational immunogen design can generate optimized immunogens that elicit a desired humoral response. Design strategies often center on targeting conserved sites on viral glycoproteins that will ultimately confer potent neutralization. For SARS-CoV-2 (SARS-2), the surface-exposed spike glycoprotein includes a broadly conserved portion, the receptor binding motif (RBM), that is required to engage the host cellular receptor, ACE2. Expanding humoral responses to this site may result in a more potent neutralizing antibody response against diverse sarbecoviruses. Here, we used a "resurfacing" approach and iterative design cycles to graft the SARS-2 RBM onto heterologous sarbecovirus scaffolds. The scaffolds were selected to vary the antigenic distance relative to SARS-2 to potentially focus responses to RBM. Multimerized versions of these immunogens elicited broad neutralization against sarbecoviruses in the context of preexisting SARS-2 immunity. These validated engineering approaches can help inform future immunogen design efforts for sarbecoviruses and are generally applicable to other viruses.

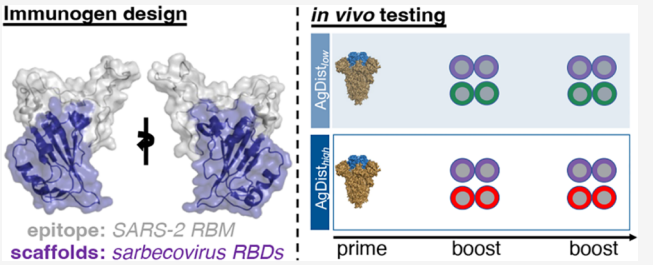

KEYWORDS: *SARS-CoV-2, coronavirus, immune imprinting*

The emergence of SARS-CoV-2 (SARS-2) highlighted the need to leverage existing, as well as new, vaccine platforms to counter novel pathogens.[1,2] Current SARS-2 vaccines have predominantly used a prefusion-stabilized version of its surface glycoprotein, spike, which is effective against both the original USA-WA1/2020 strain and subsequent variants (e.g., B.1.1.7, BA.5).[3,4] This general approach for stabilizing a viral glycoprotein was first demonstrated for influenza hemagglutinin by introducing non-native cysteines or prolines to covalently "staple" or stabilize, respectively, the prefusion state.[5,6] Prefusion stabilization was extended to viral glycoproteins from multiple viruses including other coronaviruses, respiratory syncytial virus, HIV, measles, Ebola, and Marburg.[2,7−11] This illustrates how structural knowledge informs rational immunogen design for next-generation viral vaccines against emerging pathogens.[12]

An additional approach used in structure-guided immunogen design is epitope scaffolding or "resurfacing" where a viral epitope is grafted on a comparatively unrelated protein scaffold.[12−16] These scaffolds are often based on antigenically distinct but structurally related viral proteins, as well as de novo designed scaffolds; the latter approach represents a considerable design hurdle especially when the grafted epitope is complex or conformation-specific.[15,17,18] However, when using related viral proteins as potential scaffolds, sequence identity outside the grafted epitope may influence the immune focusing effect by eliciting memory responses to additional epitopes within the scaffold. In the design process, this concern must be weighed against the engineering hurdles in a de novo designed scaffold that accurately recapitulates the conformation of the grafted epitope.

This engineering approach is particularly useful in the context of prior humoral immunity as the designed immunogens, in theory, should recall potential memory responses imprinted to the displayed epitope. Indeed, prior humoral responses are often strain-specific and are recalled at the expense of more broadly protective responses.[19−21] However, in vivo evaluation of engineered immunogens often occurs in naïve animal models, which fails to recapitulate complex immune histories observed in humans.[22−30] While it is not possible to accurately encompass the entire diversity of immune histories in animal models, it remains critical to test immunogens within the context of some preexisting immunity. This is particularly necessary when the goal is to elicit broadly

Received: September 11, 2023
Revised: January 4, 2024
Accepted: January 4, 2024
Published: January 28, 2024

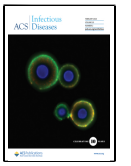

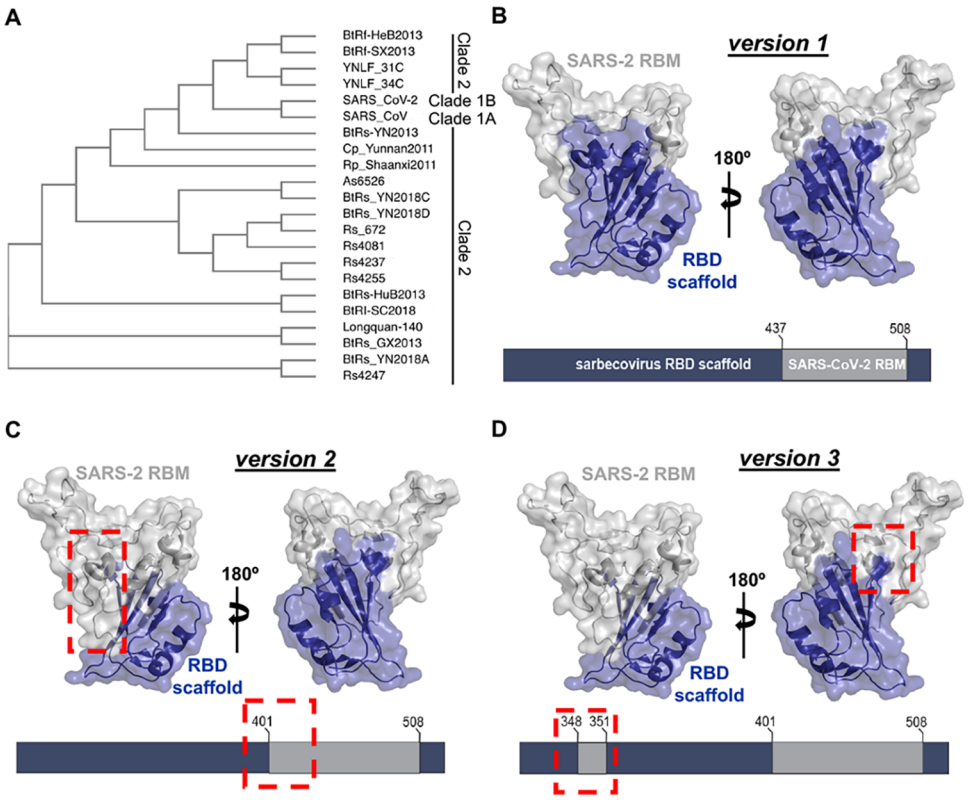

Figure 1. Selection of scaffolds and design. (A) Phylogenetic tree of 20 selected receptor binding domains used in this study; SARS-CoV and SARS-CoV-2 are included for reference. Design schematic of versions 1 (B), 2 (C), and 3 (D) resurfaced constructs, depicting RBM grafts (gray) on heterologous coronavirus scaffolds (indigo). Red dashed boxes indicate differences relative to version 1. (PDB 6M0J).

reactive responses that may be subdominant, relative to other more strain-specific responses in the imprinted repertoire. Thus, it is necessary to understand the parameters that govern the antigenicity and immunogenicity of the engineered immunogens to maximize the recall of broadly protective responses to the grafted epitopes.

Here, we engineered protein constructs that included an antigenically distinct but structurally related heterologous sarbecovirus receptor binding domain (RBD) "scaffold" onto which we "grafted" the receptor binding motif (RBM) from SARS-2. We refer to these as "resurfaced" immunogens consistent with our previous work for sarbecoviruses[14] and prior work for influenza[31] but note that "chimeric" immunogens would also suffice. The RBM is a known target of broadly neutralizing antibodies and eliciting humoral responses to this epitope may provide broad-spectrum sarbecovirus immunity.[14,32,33] In prior work, we successfully grafted the SARS-2 RBM onto SARS-1 and WIV1 RBD scaffolds.[14] These immunogens were then hyperglycosylated to preferentially shield non-RBM epitopes from immune recognition, and boosting with these immunogens in the context of prior SARS-2 immunity successfully focused immune responses to the SARS-2 RBM. Here, we specifically selected sarbecovirus RBD scaffolds with increasing antigenic diversity, relative to SARS-2, to interrogate the relationship between varying antigenic distance and the subsequent humoral response toward the grafted, RBM epitope. Importantly, we performed these studies in a murine model previously immunized with the SARS-2 spike to simulate imprinted humoral immunity. Briefly, we identified additional sarbecovirus RBD scaffolds that accepted the SARS-2 RBM graft to increase the antigenic distance between the scaffolds but determined that further variance may be required for enhanced RBM immune focusing. These data show the importance of antigenic diversity in scaffold selection and how further iterations of this design approach may lead to next-generation sarbecovirus vaccines. Moreover, it serves as a generalizable strategy for other pathogens where potential imprinted subdominant responses need to be recalled and expanded.

RESULTS

Both wild-type sarbecovirus and engineered RBDs elicit a broadly neutralizing antibody response.[14,24] For the former, the response focused on portions of the RBD outside of the RBM; this was rather expected given that the non-RBM portions of the RBDs are conserved across the different sarbecoviruses.[14] Grafting the conserved SARS-2 RBM onto heterologous sarbecovirus scaffolds would potentially alter this pattern, as the grafted RBM would be a single consistent, conserved epitope, relative to the remainder of the RBD. Thus, using multiple heterologous, antigenically distinct, sarbecovirus scaffolds "resurfaced" with the SARS-2 RBM would immune focus to this grafted epitope.

We identified 20 distinct heterologous sarbecovirus RBDs to serve as potential scaffolds for the SARS-2 RBM (Figure 1A). These scaffolds were selected from clade 2 of the sarbecovirus subgenus and are more antigenically distinct than our previously used scaffolds based on the SARS-CoV (SARS-1) and WIV1 sarbecoviruses.[14] The clade 2 members were predominantly isolated from bats in southeast Asia, and these viruses are reported not to use ACE2 as a host receptor.[33,34]

https://doi.org/10.1021/acsinfecdis.3c00483
ACS Infect. Dis. 2024, 10, 553−561

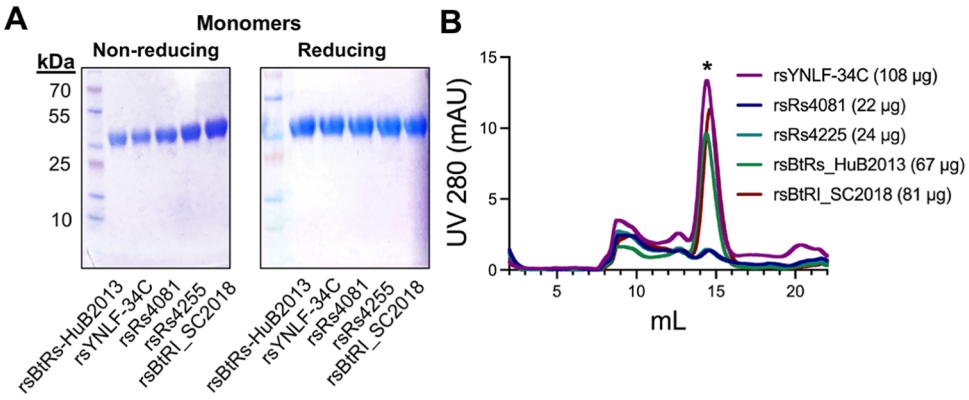

Figure 2. Resurfaced monomeric immunogen expression. (A) SDS-PAGE analysis of v2 monomers under nonreducing and reducing conditions. (B) Representative size exclusion trace with (*) marking the v2 monomeric constructs. Fractions in this peak were pooled for further characterization. Construct-specific protein yield for a 25 mL Expi293 transfection is shown in parentheses.

A

Fab	K_D
B38	~1.4 μM
CR3022	no binding
S309	no binding

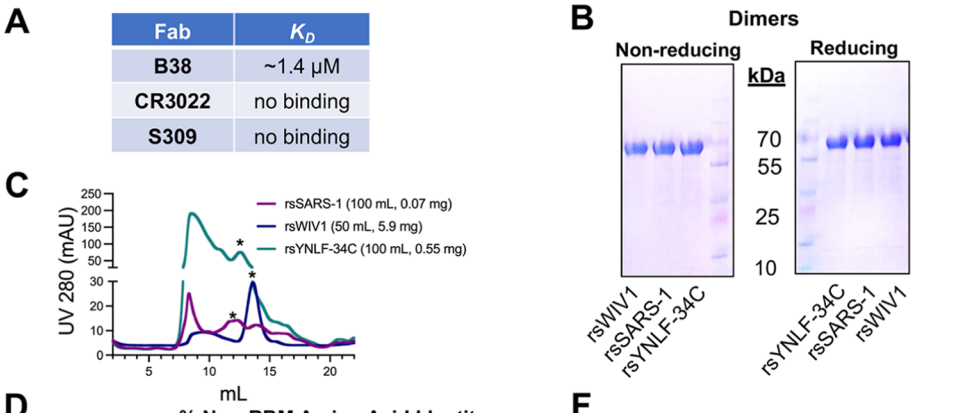

D

% Non-RBM Amino Acid Identity

	SARS-2	SARS-1	WIV1	YNLF-34C
SARS-2		85.0	87.1	80.0
SARS-1	85.0		95.0	79.3
WIV1	87.1	95.0		81.4
YNLF-34C	80.0	79.3	81.4	

E

% RBM Amino Acid Identity

	SARS-2	SARS-1	WIV1	YNLF-34C
SARS-2		49.3	52.1	36.7
SARS-1	49.3		92.9	30.4
WIV1	52.1	92.9		33.9
YNLF-34C	36.7	30.4	33.9	

F

Construct	T_m (°C)
SARS-2 Monomer	51.55±0.06
SARS-2 Dimer	48.86±0.02
rsSARS-1 Dimer	55.48±0.17
rsWIV1 Dimer	49.07±0.02
rsYNLF-34C Dimer	55.94±0.04

Figure 3. Resurfaced dimeric immunogen design and expression. (A) RBM-directed Fab B38 was used to confirm the conformational integrity of the SARS-2 RBM grafted onto rsYNLF-34C. FAB2G sensors were used with immobilized Fab to measure binding via BLI to rsYNLF-34C at 10, 5, 1, and 0.5 μM. Binding of CR3022 and S309 Fabs to rsYNLF-34C at 10 μM was also assayed, but no binding was detected. (B) SDS-PAGE analysis of dimers under nonreducing and reducing conditions. (C) Representative size exclusion trace with (*) marking the dimeric constructs. Fractions in this peak were pooled for use as immunogens. Expression volume of Expi293 cells and construct-specific protein yield are shown in parentheses. (D) Pairwise comparisons of amino acid sequence identity in the non-RBM portions of selected sarbecovirus RBDs. (E) Pairwise comparisons of amino acid sequence identity in the RBM portions of selected sarbecovirus RBDs. (F) T_m values were calculated from a Two-State Boltzmann Fit for the unfolding state of each construct using nanoDSF technique.

Using a different receptor may permit additional structural differences in comparison to sarbecoviruses that use ACE2.

To graft the SARS-2 RBM onto these scaffolds, we used three different versions (v). The first, "v1", used identical RBM boundaries as our initial resurfaced "rs", rsSARS-1 and rsWIV1 constructs: residues 437−507 (SARS-2 spike numbering) (Figure 1B).[14] A second, v2, used a more extensive RBM graft spanning residues 401−507, which was shown previously to confer ACE2 binding (Figure 1C).[34] Based on additional structural analysis, our final v3 construct incorporated SARS-2 RBD residues 348−352 in the context of v2 to potentially stabilize the SARS-2 RBM in context of the heterologous scaffold (Figure 1D). This additional region of the SARS-2 RBD was selected because it is spatially adjacent to the SARS-2 RBM; the SARS-2 RBM "caps" RBD residues 348−352 and 401−437 which were subsequently incorporated into the v2 construct.

We first attempted to express the v1 constructs for 20 different clade 2 sarbecovirus RBDs. Of these 20 constructs, 5 could be recombinantly expressed in mammalian cells to varying degrees: rsBtRs-HuB2013, rsYNLF-34C, rsRs4081, rsRs4255, and rsBtRI_SC2018. However, further analysis by

https://doi.org/10.1021/acsinfecdis.3c00483
ACS Infect. Dis. 2024, 10, 553−561

size exclusion chromatography (SEC) showed that these proteins were prone to aggregation. We then expressed the v2 and v3 constructs for these five constructs to determine if extending the graft and additional stabilizing residues would enhance expression and reduce aggregation. While all five v2 constructs had increased expression relative to v1 (<5 μg per 25 mL), rsYNLF-34C had the highest expression level and was both homogeneous and monomeric as assayed by SEC (Figure 2A,B); all five v3 constructs expressed at a level between the v1 and v2 constructs (~5 to 10 μg per 25 mL). While grafting the additional v3 residues 348−352 may in theory confer stabilizing RBM and RBD scaffold contacts based on structural analysis, in practice, increasing the graft footprint may ultimately result in a less stable engineered protein; this further underscores the need for experimental validation of in silico designed constructs and the inherent obstacles of structure-based immunogen design.

We next assessed the rsYNLF-34C v2 construct for binding to conformation-specific antibodies using a biolayer interferometry (BLI). It bound SARS-2 RBM-directed Fab, B38,[35] with comparable affinity to the wild-type SARS-2, with a monomeric-monomeric K_D of ~1.4 μM (Figures 3A and S1);[14,36] however, rsYNLF-34C did not have any detectable binding to CR3022 or S309 Fabs which bind outside the RBM[37,38] (Figure 3A). This lack of sequence conservation in the non-RBM regions of rsYNLF-34C relative to that of the SARS-2 RBD suggests that such a construct may enhance RBM focusing by minimizing cross-reactive epitopes elsewhere in the RBD; we thus chose to advance this construct to test this hypothesis.

We next engineered dimeric forms of rsYNLF-34C and our original rsSARS-1 and rsWIV1 immunogens to improve immunogenicity as previously described for wild-type coronavirus RBDs.[22] The rsWIV1 construct used the "end-to-end" dimerization approach previously described,[22] where the RBD C-terminus is followed by the N-terminus of the second RBD. The rsSARS-1 and rsYNLF-34C dimers used an alternative 13 amino acid glycine-serine linker between the two RBDs to enhance construct expression, as "end-to-end" dimerized versions failed to express in sufficient quantities. These constructs were confirmed using SDS-PAGE analysis, and the dimeric species was isolated using SEC (Figure 3B,C). The rsYNLF-34C, rsSARS-1, and rsWIV1 scaffolds range in antigenic distance from ~79.3 to ~95.0% amino acid identity relative to SARS-2 within the non-RBM portion of the RBD, while the amino acid identity ranged for each wild-type RBM ranged from ~30.4 to ~92.9% (Figure 3D,E). Melting temperatures for all homodimeric immunogen constructs were measured by nano-differential scanning fluorimetry (nanoDSF). All constructs showed no evidence of aggregation, and melting temperatures were well above 37 °C, suggesting sufficient stability for use as immunogens (Figures 3F and S2).

To test if increased antigenic distance between coronavirus RBD scaffolds would enhance SARS-2 RBM focusing, we designed an immunization regimen with two different cohorts (Figure 4). The first included a cocktail of the rsSARS-1 and rsWIV1 dimers, which share 95.0% amino acid sequence identity between the scaffolds in the non-RBM portion of the RBDs and are referred to as antigenic distance "low" ($AgDist_{low}$). The second included rsYNLF-34C and rsWIV1 dimers, which have 81.4% amino acid sequence identity and are referred to as $AgDist_{high}$.

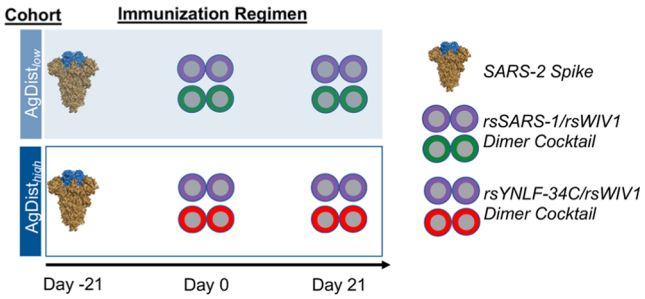

Figure 4. Antigenic distance investigation immunizations. Schematic of immunization regimens. Two immunization cohorts (n = 5 mice each) were primed with SARS-2 two-proline-stabilized (2P) spike protein on day -21 and then boosted with a cocktail of either the rsSARS-1 and rsWIV1 dimers ("$AgDist_{low}$" cohort) or the rsWIV1 and rsYNLF-34C dimers ("$AgDist_{high}$" cohort) at days 0 and 21.

We then immunized two cohorts of C57BL/6 mice that were first primed with recombinant SARS-2 spike to simulate preexisting immunity and then immunized and boosted with either $AgDist_{low}$ or $AgDist_{high}$ immunogens (Figure 5A). Serum was collected at day 35, and ELISAs were performed against a variety of coronavirus proteins. To assess potential RBM focusing, we used a previously characterized SARS-2 construct (RBM^{hg}) that has glycans placed across the RBM to abrogate binding of RBM-directed antibodies (e.g., B38).[14] Neither cohort, however, showed a significant difference in titers against the wild-type SARS-2 RBD and the SARS-2 RBM^{hg} construct, indicating a lack of serum antibody response focusing to the SARS-2 RBM. One possible explanation for these findings could be that additional antigenic diversity between scaffolds may be required to achieve serum antibody focusing to the SARS-2 RBM. Low-level reactivity of convalescent SARS-2 human subject sera was measured against the rsYNLF-34C dimeric immunogen, but this did not differ significantly from reactivity against BSA (Figure 5B). Nevertheless, this possibly suggests that the immunization of recovered human subjects with rsYNLF-34C may successfully recall limited SARS-2-directed antibody responses.

Despite the lack of observed RBM focusing, sera from the $AgDist_{high}$ cohort showed detectable neutralization against all sarbecoviruses tested (Figure 5C). This contrasts with the sera from the $AgDist_{low}$ cohort, which showed limited neutralization against the SARS-2 Omicron variant, SARS-1, and WIV1 pseudoviruses (Figure 5C). Immune focusing to conserved RBM epitopes has been previously shown to confer potent neutralization across a broad range of sarbecoviruses.[14] This pattern could be one possible explanation for these results, with some level of immune focusing in the $AgDist_{high}$ cohort that is not readily detected by ELISA.

DISCUSSION

This study builds upon our previous work that combined resurfacing and hyperglycosylation protein engineering approaches for potential immune focusing to conserved epitopes.[14] Boosting with these engineered immunogens following a SARS-2 spike prime was compared to boosting with a multimerized wild-type SARS-2 RBD, which showed no apparent immune focusing to the SARS-2 RBM and resulted in limited serum neutralization breadth across related sarbecoviruses.[14,39,40] In that study, the SARS-1 and WIV1 scaffolds had a rather high degree of sequence identity relative to each other

https://doi.org/10.1021/acsinfecdis.3c00483
ACS Infect. Dis. 2024, 10, 553−561

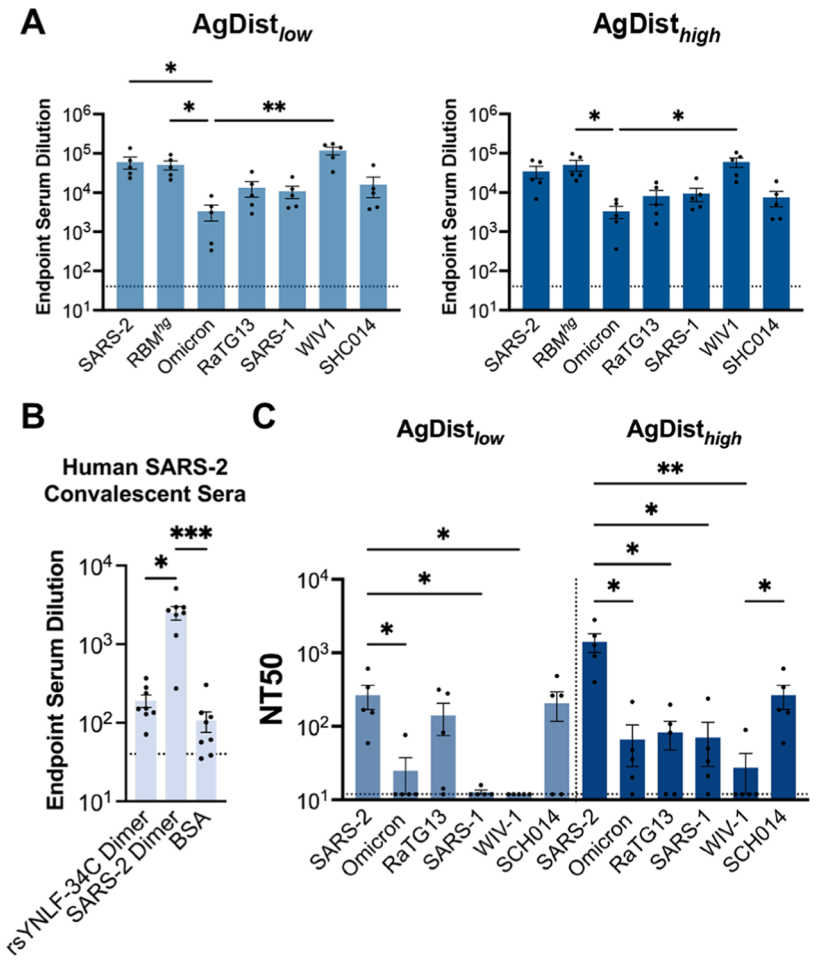

Figure 5. Antigenic distance investigation immunization serum reactivity. (A) Serum collected at day 35 was assayed in ELISA against different coronavirus antigens. (B) Human SARS-2 convalescent sera from 8 subjects were assayed in ELISA against the rsYNLF-34C homodimeric immunogen. (C) Pseudovirus neutralization was assayed against a panel of sarbecoviruses, ordered here based on spike amino acid sequence similarity to SARS-2. Statistical significance for (A, C) was determined using Kruskal–Wallis test with post hoc analysis using Dunn's test corrected for multiple comparisons (*p < 0.05, **p < 0.01, ***p < 0.001); nonsignificant comparisons not marked.

as well as to SARS-2. Here, we used our resurfacing approach to identify additional sarbecovirus RBD scaffolds that could present the SARS-2 RBM to further maximize the antigenic distance between the scaffolds. It appears, however, that further increasing this distance may still be required to achieve immune focusing. Additional investigations will be required to interrogate the exact scaffold design parameters required to achieve successful immune focusing to the grafted RBM. The extent to which the parameters determined for this resurfacing approach and scaffold identification apply to grafted epitopes from other viral epitopes, such as the influenza receptor binding site, is also of interest.

We note, however, that despite nondetectable SARS-2 RBM focusing within our assay, the AgDist$_{high}$ cohort did show improved neutralization breadth in the context of prior SARS-2 spike imprinting. This suggests that these resurfaced immunogens and approach more broadly may serve as a foundation for next-generation pan-sarbecovirus vaccines by preferentially increasing the representation of the SARS-2 RBM within candidate immunogens. Broadly neutralizing, RBM-directed antibodies have also been characterized by others.[32,33,41,42] Simply immunizing with diverse sarbecovirus RBDs does not necessarily confer broad neutralization in the setting of SARS-2 spike imprinting; however, we previously showed that three resurfaced RBDs elicited a broadly neutralizing antibody response when a cocktail of homotrimeric RBDs was used as the boosting immunogen.[14] One possible explanation is that the orientation and subsequent positioning of the RBD components in a particular immunogen might affect the extent to which cross-reactive antibodies are elicited. Indeed, this has been suggested for other immunogens, in particular those displayed on various nanoparticles or DNA-based scaffolds.[43,44]

Immunization with a range of wild-type sarbecovirus RBDs also conferred broad neutralization both in naïve animals and in the context of SARS-2 spike imprinting.[14,24] These broadly neutralizing antibodies preferentially target conserved epitopes on the SARS-2 RBD, with most contacts falling outside the RBM.[14,45] Similar findings have been demonstrated for influenza after immunization with diverse hemagglutinins.[43] We recently showed that a similar resurfacing approach for influenza showed that grafting the complex, conformation-specific, hemagglutinin receptor binding site onto multiple antigenically distinct scaffolds, could preferentially expand responses to this site.[46] Thus, our study here provides further support, with further design iterations required, that this principle of "epitope enrichment" may be broadly applicable

https://doi.org/10.1021/acsinfecdis.3c00483
ACS Infect. Dis. 2024, 10, 553−561

across virus families and could be leveraged to design immunogens that focus on any enriched epitope of interest.

The structure-guided, rational immunogen design approaches implemented in this study have the potential to inform future pan-sarbecovirus vaccine efforts. Additionally, these findings provide some mechanistic insight into parameters required to influence the humoral immune response toward desired epitopes.

METHODS

Protein Expression and Purification. Dr. Jason McLellan at the University of Texas, Austin generously shared the SARS-2 spike plasmid, which contained a Foldon trimerization domain and C-terminal HRV 3C-cleavable 6xHis and 2xStrep II tags. RBD designs were based on the following sequences: SARS-2 RBD (Genbank MN975262.1), SARS-1 RBD (Genbank ABD72970.1), WIV1 RBD (Genbank AGZ48828.1), RaTG13 RBD (Genbank QHR63300.2), and SHC014 RBD (Genbank QJE50589.1). Codon optimization was performed using Integrated DNA Technologies, and gblock constructs were purchased and cloned into the pVRC expression vector. Proteins included a C-terminal HRV 3C-cleavable 8xHis tag, as well as SBP tags in the monomeric and dimeric RBDs and a previously published hyperglycosylated, cystine-stabilized trimerization tag in the trimeric RBDs.[14]

Constructs were expressed using Expifectamine transfection reagents in Expi293F cells (Thermo Fisher) according to the manufacturer's protocol. After 5−7 days, transfections were harvested, and supernatants were purified via immobilized metal affinity chromatography using Cobalt-TALON resin (Takara). Eluted proteins were further purified by size exclusion chromatography using a Superdex 200 Increase 10/300 GL column (Cytiva) in PBS (Corning). Relevant fractions were pooled.

HRV 3C protease (Thermo Scientific) was used to remove purification tags prior to immunizations. Cleaved protein was repurified using Cobalt-TALON resin and size exclusion chromatography to separate uncleaved protein, protease, and cleaved tags from cleaved protein.

Immunizations. Immunizations were performed in C57BL/6 female mice aged 6−10 weeks (Charles River Laboratories). Each mouse received 20 μg of protein adjuvanted with 50% w/v Sigma Adjuvant System in 100 μL of inoculum via the intraperitoneal route.[47] The intraperitoneal route was chosen to capitalize on the antigen drainage to the spleen. Immunizations occurred at days −21, 0, and 21, with serum characterization occurring with day 35 samples. All experiments were conducted with institutional IACUC approval (MGH protocol 2014N000252).

Human Serum Samples. Serum samples from eight convalescent, unvaccinated human subjects were collected as previously described and had been characterized in this prior publication.[48] Use of patient samples was approved by the Partners Institutional Review Board (protocol 2020P000895).

Serum ELISAs. Serum ELISAs were performed as previously described.[14] Briefly, plates were coated with 100 μL of protein at 5 μg/mL overnight at 4 °C, then blocked with 150 μL of 1% BSA in PBS-Tween for 1 h at room temperature. Sera was added at a starting dilution of 1:40 with a serial 5-fold dilution and incubated for 90 min at room temperature. Plates were washed, and 150 μL of HRP-conjugated antimouse IgG (Abcam) or HRP-conjugated antihuman IgG (Abcam) was added at 1:20,000. After a 1 h secondary incubation at room temperature, the plates were washed and 150 μL of 1× ABTS development solution (Thermo Fisher) was added. Plates were developed for 30 min at room temperature before stopping with 100 μL of 1% SDS to read on a SpectraMaxiD3 plate reader (Molecular Devices) for absorbance at 405 nm.

Pseudovirus Neutralization Assay. Serum pseudovirus neutralization assays were performed as previously described.[14,49] Briefly, pseudotyped lentiviral particles were generated via transient transfection of 293T cells and tittered using 293T-ACE2 cells[50] and the HIV-1 p24CA antigen capture assay (Leidos Biomedical Research, Inc.). Assays were performed using a Tecan Fluent Automated Workstation and 384-well plates (Grenier), and sera were initially diluted 1:3 with subsequent serial 3-fold dilutions. Each well received 20 μL each of sera and pseudovirus (125 infectious units), and plates were incubated 1 h at room temperature. 10,000 293T-ACE2 cells[50] in 20 μL of media with 15 μg/mL Polybrene was added, and additional incubation occurred at 37 °C for 60−72 h. Cells were lysed,[51] and luciferase expression was quantified on a Spectramax L luminometer (Molecular Devices). Neutralization percentage was calculated for each serum concentration by deducting background luminescence from cells-only wells and dividing by the luminescence of wells containing cells and virus. GraphPad Prism (version 9) was used to fit nonlinear regressions, and IC50 values were calculated for samples with neutralization values that were at least 80% at the maximum serum concentration. Reciprocal IC50 values were used to obtain the NT50 values.

Melting Temperatures. Nano-differential scanning fluorimetry (nanoDSF) was performed on a Prometheus NT.Plex instrument from NanoTemper. Prepared samples were transferred to a 384-well plate and loaded into NanoTemper NT.Plex Capillary Chips. The experiment was performed in a replicate of 2. Samples were heated from 20 to 95 °C at a rate of 1.5 °C/min. Data were collected by using NanoTemper PR.ThermControl software.

ASSOCIATED CONTENT

Data Availability Statement

The data sets generated and analyzed during the study are available from the corresponding author.

Supporting Information

The Supporting Information is available free of charge at https://pubs.acs.org/doi/10.1021/acsinfecdis.3c00483.

Raw biolayer interferometry curves for B38 Fab binding to rsYNLF-34C RBD and raw nanoDSF data for immunogens (PDF)

AUTHOR INFORMATION

Corresponding Author

Aaron G. Schmidt − *Ragon Institute of Mass General, MIT, and Harvard, Cambridge, Massachusetts 02139, United States; Department of Microbiology, Harvard Medical School, Boston, Massachusetts 02115, United States;* orcid.org/0000-0003-3627-2553; Phone: 857-268-7118; Email: aschmidt@crystal.harvard.edu

Authors

Blake M. Hauser − *Ragon Institute of Mass General, MIT, and Harvard, Cambridge, Massachusetts 02139, United States*

Maya Sangesland − *Ragon Institute of Mass General, MIT, and Harvard, Cambridge, Massachusetts 02139, United States*
Evan C. Lam − *Ragon Institute of Mass General, MIT, and Harvard, Cambridge, Massachusetts 02139, United States*
Kerri J. St Denis − *Ragon Institute of Mass General, MIT, and Harvard, Cambridge, Massachusetts 02139, United States*
Maegan L. Sheehan − *Ragon Institute of Mass General, MIT, and Harvard, Cambridge, Massachusetts 02139, United States*
Mya L. Vu − *Ragon Institute of Mass General, MIT, and Harvard, Cambridge, Massachusetts 02139, United States*
Agnes H. Cheng − *Ragon Institute of Mass General, MIT, and Harvard, Cambridge, Massachusetts 02139, United States*
Sophia Sordilla − *Ragon Institute of Mass General, MIT, and Harvard, Cambridge, Massachusetts 02139, United States*
Dana Thornlow Lamson − *Ragon Institute of Mass General, MIT, and Harvard, Cambridge, Massachusetts 02139, United States; Department of Microbiology, Harvard Medical School, Boston, Massachusetts 02115, United States*
Ahmad W. Almawi − *Center for Molecular Interactions, Department of Biological Chemistry and Molecular Pharmacology, Harvard Medical School, Boston, Massachusetts 02115, United States*
Alejandro B. Balazs − *Ragon Institute of Mass General, MIT, and Harvard, Cambridge, Massachusetts 02139, United States*
Daniel Lingwood − *Ragon Institute of Mass General, MIT, and Harvard, Cambridge, Massachusetts 02139, United States;* orcid.org/0000-0001-5631-9238

Complete contact information is available at: https://pubs.acs.org/10.1021/acsinfecdis.3c00483

Author Contributions

Conceptualization, B.M.H., A.G.S.; Methodology, B.M.H., M.S., E.C.L., A.G.S.; Investigation, B.M.H., M.S., E.C.L., K.J.S.D., M.L.S., M.L.V., A.H.C.; Writing—original draft, B.M.H. and A.G.S.; Writing—review and editing, all authors; Funding acquisition, A.B.B., D.L., A.G.S.; Supervision, A.B.B., D.L., A.G.S.

Notes

The authors declare no competing financial interest.

■ ACKNOWLEDGMENTS

The authors thank Dr. Jason McLellan from University of Texas, Austin for the spike plasmid. They also thank Nir Hacohen and Michael Farzan for the kind gift of the ACE2 expressing 293T cells and the Center for Macromolecular Interactions at Harvard Medical School for experimental support specifically, Kelly Arnett . The authors acknowledge funding from NIH R01s AI146779 (A.G.S); AI174875 (A.B.B.); AI155447, AI137057, and AI153098 (D.L.); a Massachusetts Consortium on Pathogenesis Readiness (MassCPR) grant (A.G.S. and A.B.B.); NIH P01 AI168347 (A.G.S.); training grants: NIGMS T32 GM007753 (B.M.H.), F31 Al138368 (M.S.), F30 AI160908 (B.M.H.). ABB. National Institutes for Drug Abuse (NIDA) Avenir New Innovator Award DP2DA040254 (A.B.B.) and CDC subcontract 200-2016-91773-T.O.2 (A.B.B.)

■ REFERENCES

(1) Corbett, K. S.; Edwards, D. K.; Leist, S. R.; Abiona, O. M.; Boyoglu-Barnum, S.; Gillespie, R. A.; Himansu, S.; Schafer, A.; Ziwawo, C. T.; DiPiazza, A. T.; Dinnon, K. H.; Elbashir, S. M.; Shaw, C. A.; Woods, A.; Fritch, E. J.; Martinez, D. R.; Bock, K. W.; Minai, M.; Nagata, B. M.; Hutchinson, G. B.; Wu, K.; Henry, C.; Bahl, K.; Garcia-Dominguez, D.; Ma, L.; Renzi, I.; Kong, W. P.; Schmidt, S. D.; Wang, L.; Zhang, Y.; Phung, E.; Chang, L. A.; Loomis, R. J.; Altaras, N. E.; Narayanan, E.; Metkar, M.; Presnyak, V.; Liu, C.; Louder, M. K.; Shi, W.; Leung, K.; Yang, E. S.; West, A.; Gully, K. L.; Stevens, L. J.; Wang, N.; Wrapp, D.; Doria-Rose, N. A.; Stewart-Jones, G.; Bennett, H.; Alvarado, G. S.; Nason, M. C.; Ruckwardt, T. J.; McLellan, J. S.; Denison, M. R.; Chappell, J. D.; Moore, I. N.; Morabito, K. M.; Mascola, J. R.; Baric, R. S.; Carfi, A.; Graham, B. S. SARS-CoV-2 mRNA vaccine design enabled by prototype pathogen preparedness. *Nature* **2020**, *586* (7830), 567−571.
(2) Pallesen, J.; Wang, N.; Corbett, K. S.; Wrapp, D.; Kirchdoerfer, R. N.; Turner, H. L.; Cottrell, C. A.; Becker, M. M.; Wang, L.; Shi, W.; Kong, W. P.; Andres, E. L.; Kettenbach, A. N.; Denison, M. R.; Chappell, J. D.; Graham, B. S.; Ward, A. B.; McLellan, J. S. Immunogenicity and structures of a rationally designed prefusion MERS-CoV spike antigen. *Proc. Natl. Acad. Sci. U.S.A.* **2017**, *114* (35), E7348−E7357, DOI: 10.1073/pnas.1707304114.
(3) Garcia-Beltran, W. F.; St Denis, K. J.; Hoelzemer, A.; Lam, E. C.; Nitido, A. D.; Sheehan, M. L.; Berrios, C.; Ofoman, O.; Chang, C. C.; Hauser, B. M.; Feldman, J.; Roederer, A. L.; Gregory, D. J.; Poznansky, M. C.; Schmidt, A. G.; Iafrate, A. J.; Naranbhai, V.; Balazs, A. B. mRNA-based COVID-19 vaccine boosters induce neutralizing immunity against SARS-CoV-2 Omicron variant. *Cell* **2022**, *185* (3), 457−466.e4, DOI: 10.1016/j.cell.2021.12.033.
(4) Nanduri, S.; Pilishvili, T.; Derado, G.; Soe, M. M.; Dollard, P.; Wu, H.; Li, Q.; Bagchi, S.; Dubendris, H.; Link-Gelles, R.; Jernigan, J. A.; Budnitz, D.; Bell, J.; Benin, A.; Shang, N.; Edwards, J. R.; Verani, J. R.; Schrag, S. J. Effectiveness of Pfizer-BioNTech and Moderna Vaccines in Preventing SARS-CoV-2 Infection Among Nursing Home Residents Before and During Widespread Circulation of the SARS-CoV-2 B.1.617.2 (Delta) Variant - National Healthcare Safety Network, March 1-August 1, 2021. *MMWR Morb. Mortal. Wkly. Rep.* **2021**, *70* (34), 1163−1166.
(5) Lee, P. S.; Zhu, X.; Yu, W.; Wilson, I. A. Design and Structure of an Engineered Disulfide-Stabilized Influenza Virus Hemagglutinin Trimer. *J. Virol.* **2015**, *89* (14), 7417−7420.
(6) Xu, R.; McBride, R.; Nycholat, C. M.; Paulson, J. C.; Wilson, I. A. Structural characterization of the hemagglutinin receptor specificity from the 2009 H1N1 influenza pandemic. *J. Virol.* **2012**, *86* (2), 982−990.
(7) Wrapp, D.; Wang, N.; Corbett, K. S.; Goldsmith, J. A.; Hsieh, C. L.; Abiona, O.; Graham, B. S.; McLellan, J. S. Cryo-EM structure of the 2019-nCoV spike in the prefusion conformation. *Science* **2020**, *367* (6483), 1260−1263.
(8) McLellan, J. S.; Chen, M.; Joyce, M. G.; Sastry, M.; Stewart-Jones, G. B.; Yang, Y.; Zhang, B.; Chen, L.; Srivatsan, S.; Zheng, A.; Zhou, T.; Graepel, K. W.; Kumar, A.; Moin, S.; Boyington, J. C.; Chuang, G. Y.; Soto, C.; Baxa, U.; Bakker, A. Q.; Spits, H.; Beaumont, T.; Zheng, Z.; Xia, N.; Ko, S. Y.; Todd, J. P.; Rao, S.; Graham, B. S.; Kwong, P. D. Structure-based design of a fusion glycoprotein vaccine for respiratory syncytial virus. *Science* **2013**, *342* (6158), 592−598.
(9) Lee, J. K.; Prussia, A.; Snyder, J. P.; Plemper, R. K. Reversible inhibition of the fusion activity of measles virus F protein by an engineered intersubunit disulfide bridge. *J. Virol.* **2007**, *81* (16), 8821−8826.
(10) Sanders, R. W.; Derking, R.; Cupo, A.; Julien, J. P.; Yasmeen, A.; de Val, N.; Kim, H. J.; Blattner, C.; de la Pena, A. T.; Korzun, J.; Golabek, M.; de Los Reyes, K.; Ketas, T. J.; van Gils, M. J.; King, C. R.; Wilson, I. A.; Ward, A. B.; Klasse, P. J.; Moore, J. P. A next-generation cleaved, soluble HIV-1 Env trimer, BG505 SOSIP.664 gp140, expresses multiple epitopes for broadly neutralizing but not non-neutralizing antibodies. *PLoS Pathog.* **2013**, *9* (9), No. e1003618.

(11) Rutten, L.; Gilman, M. S. A.; Blokland, S.; Juraszek, J.; McLellan, J. S.; Langedijk, J. P. M. Structure-Based Design of Prefusion-Stabilized Filovirus Glycoprotein Trimers. *Cell Rep.* **2020**, *30* (13), 4540−4550.e3, DOI: 10.1016/j.celrep.2020.03.025.
(12) Caradonna, T. M.; Schmidt, A. G. Protein engineering strategies for rational immunogen design. *npj Vaccines* **2021**, *6* (1), No. 154, DOI: 10.1038/s41541-021-00417-1.
(13) Bajic, G.; Maron, M. J.; Caradonna, T. M.; Tian, M.; Mermelstein, A.; Fera, D.; Kelsoe, G.; Kuraoka, M.; Schmidt, A. G. Structure-Guided Molecular Grafting of a Complex Broadly Neutralizing Viral Epitope. *ACS Infect. Dis.* **2020**, *6* (5), 1182−1191.
(14) Hauser, B. M.; Sangesland, M.; St Denis, K. J.; Lam, E. C.; Case, J. B.; Windsor, I. W.; Feldman, J.; Caradonna, T. M.; Kannegieter, T.; Diamond, M. S.; Balazs, A. B.; Lingwood, D.; Schmidt, A. G. Rationally designed immunogens enable immune focusing following SARS-CoV-2 spike imprinting. *Cell Rep.*. **2022**, *38* (12), No. 110561, DOI: 10.1016/j.celrep.2022.110561.
(15) Ofek, G.; Guenaga, F. J.; Schief, W. R.; Skinner, J.; Baker, D.; Wyatt, R.; Kwong, P. D. Elicitation of structure-specific antibodies by epitope scaffolds. *Proc. Natl. Acad. Sci. U. S. A.* **2010**, *107* (42), 17880−17887.
(16) Correia, B. E.; Bates, J. T.; Loomis, R. J.; Baneyx, G.; Carrico, C.; Jardine, J. G.; Rupert, P.; Correnti, C.; Kalyuzhniy, O.; Vittal, V.; Connell, M. J.; Stevens, E.; Schroeter, A.; Chen, M.; Macpherson, S.; Serra, A. M.; Adachi, Y.; Holmes, M. A.; Li, Y.; Klevit, R. E.; Graham, B. S.; Wyatt, R. T.; Baker, D.; Strong, R. K.; Crowe, J. E., Jr; Johnson, P. R.; Schief, W. R. Proof of principle for epitope-focused vaccine design. *Nature* **2014**, *507* (7491), 201−206.
(17) MacDonald, J. T.; Maksimiak, K.; Sadowski, M. I.; Taylor, W. R. De novo backbone scaffolds for protein design. *Proteins* **2010**, *78* (5), 1311−1325.
(18) Azoitei, M. L.; Ban, Y. E.; Julien, J. P.; Bryson, S.; Schroeter, A.; Kalyuzhniy, O.; Porter, J. R.; Adachi, Y.; Baker, D.; Pai, E. F.; Schief, W. R. Computational design of high-affinity epitope scaffolds by backbone grafting of a linear epitope. *J. Mol. Biol.* **2012**, *415* (1), 175−192.
(19) Guthmiller, J. J.; Wilson, P. C. Harnessing immune history to combat influenza viruses. *Curr. Opin. Immunol.* **2018**, *53*, 187−195.
(20) Wheatley, A. K.; Fox, A.; Tan, H. X.; Juno, J. A.; Davenport, M. P.; Subbarao, K.; Kent, S. J. Immune imprinting and SARS-CoV-2 vaccine design. *Trends Immunol.* **2021**, *42* (11), 956−959.
(21) Roltgen, K.; Nielsen, S. C. A.; Silva, O.; Younes, S. F.; Zaslavsky, M.; Costales, C.; Yang, F.; Wirz, O. F.; Solis, D.; Hoh, R. A.; Wang, A.; Arunachalam, P. S.; Colburg, D.; Zhao, S.; Haraguchi, E.; Lee, A. S.; Shah, M. M.; Manohar, M.; Chang, I.; Gao, F.; Mallajosyula, V.; Li, C.; Liu, J.; Shoura, M. J.; Sindher, S. B.; Parsons, E.; Dashdorj, N. J.; Dashdorj, N. D.; Monroe, R.; Serrano, G. E.; Beach, T. G.; Chinthrajah, R. S.; Charville, G. W.; Wilbur, J. L.; Wohlstadter, J. N.; Davis, M. M.; Pulendran, B.; Troxell, M. L.; Sigal, G. B.; Natkunam, Y.; Pinsky, B. A.; Nadeau, K. C.; Boyd, S. D. Immune imprinting, breadth of variant recognition, and germinal center response in human SARS-CoV-2 infection and vaccination. *Cell* **2022**, *185* (6), 1025−1040.e14, DOI: 10.1016/j.cell.2022.01.018.
(22) Dai, L.; Zheng, T.; Xu, K.; Han, Y.; Xu, L.; Huang, E.; An, Y.; Cheng, Y.; Li, S.; Liu, M.; Yang, M.; Li, Y.; Cheng, H.; Yuan, Y.; Zhang, W.; Ke, C.; Wong, G.; Qi, J.; Qin, C.; Yan, J.; Gao, G. F. A Universal Design of Betacoronavirus Vaccines against COVID-19, MERS, and SARS. *Cell* **2020**, *182* (3), 722−733.e11, DOI: 10.1016/j.cell.2020.06.035.
(23) Saunders, K. O.; Lee, E.; Parks, R.; Martinez, D. R.; Li, D.; Chen, H.; Edwards, R. J.; Gobeil, S.; Barr, M.; Mansouri, K.; Alam, S. M.; Sutherland, L. L.; Cai, F.; Sanzone, A. M.; Berry, M.; Manne, K.; Bock, K. W.; Minai, M.; Nagata, B. M.; Kapingidza, A. B.; Azoitei, M.; Tse, L. V.; Scobey, T. D.; Spreng, R. L.; Rountree, R. W.; DeMarco, C. T.; Denny, T. N.; Woods, C. W.; Petzold, E. W.; Tang, J.; Oguin, T. H., 3rd; Sempowski, G. D.; Gagne, M.; Douek, D. C.; Tomai, M. A.; Fox, C. B.; Seder, R.; Wiehe, K.; Weissman, D.; Pardi, N.; Golding, H.; Khurana, S.; Acharya, P.; Andersen, H.; Lewis, M. G.; Moore, I. N.; Montefiori, D. C.; Baric, R. S.; Haynes, B. F. Neutralizing antibody vaccine for pandemic and pre-emergent coronaviruses. *Nature* **2021**, *594* (7864), 553−559.
(24) Cohen, A. A.; Gnanapragasam, P. N. P.; Lee, Y. E.; Hoffman, P. R.; Ou, S.; Kakutani, L. M.; Keeffe, J. R.; Wu, H. J.; Howarth, M.; West, A. P.; Barnes, C. O.; Nussenzweig, M. C.; Bjorkman, P. J. Mosaic nanoparticles elicit cross-reactive immune responses to zoonotic coronaviruses in mice. *Science* **2021**, *371* (6530), 735−741.
(25) Walls, A. C.; Fiala, B.; Schafer, A.; Wrenn, S.; Pham, M. N.; Murphy, M.; Tse, L. V.; Shehata, L.; O'Connor, M. A.; Chen, C.; Navarro, M. J.; Miranda, M. C.; Pettie, D.; Ravichandran, R.; Kraft, J. C.; Ogohara, C.; Palser, A.; Chalk, S.; Lee, E. C.; Guerriero, K.; Kepl, E.; Chow, C. M.; Sydeman, C.; Hodge, E. A.; Brown, B.; Fuller, J. T.; Dinnon, K. H., 3rd; Gralinski, L. E.; Leist, S. R.; Gully, K. L.; Lewis, T. B.; Guttman, M.; Chu, H. Y.; Lee, K. K.; Fuller, D. H.; Baric, R. S.; Kellam, P.; Carter, L.; Pepper, M.; Sheahan, T. P.; Veesler, D.; King, N. P. Elicitation of Potent Neutralizing Antibody Responses by Designed Protein Nanoparticle Vaccines for SARS-CoV-2. *Cell* **2020**, *183* (5), 1367−1382.e17, DOI: 10.1016/j.cell.2020.10.043.
(26) Ma, X.; Zou, F.; Yu, F.; Li, R.; Yuan, Y.; Zhang, Y.; Zhang, X.; Deng, J.; Chen, T.; Song, Z.; Qiao, Y.; Zhan, Y.; Liu, J.; Zhang, J.; Zhang, X.; Peng, Z.; Li, Y.; Lin, Y.; Liang, L.; Wang, G.; Chen, Y.; Chen, Q.; Pan, T.; He, X.; Zhang, H. Nanoparticle Vaccines Based on the Receptor Binding Domain (RBD) and Heptad Repeat (HR) of SARS-CoV-2 Elicit Robust Protective Immune Responses. *Immunity* **2020**, *53* (6), 1315−1330.e9, DOI: 10.1016/j.immuni.2020.11.015.
(27) Wang, W.; Huang, B.; Zhu, Y.; Tan, W.; Zhu, M. Ferritin nanoparticle-based SARS-CoV-2 RBD vaccine induces a persistent antibody response and long-term memory in mice. *Cell Mol. Immunol.* **2021**, *18* (3), 749−751.
(28) Kang, Y. F.; Sun, C.; Zhuang, Z.; Yuan, R. Y.; Zheng, Q.; Li, J. P.; Zhou, P. P.; Chen, X. C.; Liu, Z.; Zhang, X.; Yu, X. H.; Kong, X. W.; Zhu, Q. Y.; Zhong, Q.; Xu, M.; Zhong, N. S.; Zeng, Y. X.; Feng, G. K.; Ke, C.; Zhao, J. C.; Zeng, M. S. Rapid Development of SARS-CoV-2 Spike Protein Receptor-Binding Domain Self-Assembled Nanoparticle Vaccine Candidates. *ACS Nano* **2021**, *15* (2), 2738−2752.
(29) Li, H.; Guo, L.; Zheng, H.; Li, J.; Zhao, X.; Li, J.; Liang, Y.; Yang, F.; Zhao, Y.; Yang, J.; Xue, M.; Zuo, Y.; Zhou, J.; Chen, Y.; Yang, Z.; Li, Y.; Jin, W.; Shi, H.; He, Z.; Li, Q.; Liu, L. Self-Assembling Nanoparticle Vaccines Displaying the Receptor Binding Domain of SARS-CoV-2 Elicit Robust Protective Immune Responses in Rhesus Monkeys. *Bioconjugate Chem.* **2021**, *32* (5), 1034−1046.
(30) Shinnakasu, R.; Sakakibara, S.; Yamamoto, H.; Wang, P. H.; Moriyama, S.; Sax, N.; Ono, C.; Yamanaka, A.; Adachi, Y.; Onodera, T.; Sato, T.; Shinkai, M.; Suzuki, R.; Matsuura, Y.; Hashii, N.; Takahashi, Y.; Inoue, T.; Yamashita, K.; Kurosaki, T. Glycan engineering of the SARS-CoV-2 receptor-binding domain elicits cross-neutralizing antibodies for SARS-related viruses. *J. Exp. Med.* **2021**, *218* (12), No. e20211003, DOI: 10.1084/jem.20211003.
(31) Krammer, F.; Pica, N.; Hai, R.; Margine, I.; Palese, P. Chimeric hemagglutinin influenza virus vaccine constructs elicit broadly protective stalk-specific antibodies. *J. Virol.* **2013**, *87* (12), 6542−6550.
(32) Rappazzo, C. G.; Tse, L. V.; Kaku, C. I.; Wrapp, D.; Sakharkar, M.; Huang, D.; Deveau, L. M.; Yockachonis, T. J.; Herbert, A. S.; Battles, M. B.; O'Brien, C. M.; Brown, M. E.; Geoghegan, J. C.; Belk, J.; Peng, L.; Yang, L.; Hou, Y.; Scobey, T. D.; Burton, D. R.; Nemazee, D.; Dye, J. M.; Voss, J. E.; Gunn, B. M.; McLellan, J. S.; Baric, R. S.; Gralinski, L. E.; Walker, L. M. Broad and potent activity against SARS-like viruses by an engineered human monoclonal antibody. *Science* **2021**, *371* (6531), 823−829.
(33) Wec, A. Z.; Wrapp, D.; Herbert, A. S.; Maurer, D. P.; Haslwanter, D.; Sakharkar, M.; Jangra, R. K.; Dieterle, M. E.; Lilov, A.; Huang, D.; Tse, L. V.; Johnson, N. V.; Hsieh, C. L.; Wang, N.; Nett, J. H.; Champney, E.; Burnina, I.; Brown, M.; Lin, S.; Sinclair, M.; Johnson, C.; Pudi, S.; Bortz, R., 3rd; Wirchnianski, A. S.; Laudermilch, E.; Florez, C.; Fels, J. M.; O'Brien, C. M.; Graham, B. S.; Nemazee, D.; Burton, D. R.; Baric, R. S.; Voss, J. E.; Chandran, K.; Dye, J. M.; McLellan, J. S.; Walker, L. M. Broad neutralization of SARS-related

viruses by human monoclonal antibodies. *Science* **2020**, *369*, 731−736, DOI: 10.1126/science.abc7424.
(34) Letko, M.; Marzi, A.; Munster, V. Functional assessment of cell entry and receptor usage for SARS-CoV-2 and other lineage B betacoronaviruses. *Nat. Microbiol.* **2020**, *5* (4), 562−569.
(35) Wu, Y.; Wang, F.; Shen, C.; Peng, W.; Li, D.; Zhao, C.; Li, Z.; Li, S.; Bi, Y.; Yang, Y.; Gong, Y.; Xiao, H.; Fan, Z.; Tan, S.; Wu, G.; Tan, W.; Lu, X.; Fan, C.; Wang, Q.; Liu, Y.; Zhang, C.; Qi, J.; Gao, G. F.; Gao, F.; Liu, L. A noncompeting pair of human neutralizing antibodies block COVID-19 virus binding to its receptor ACE2. *Science* **2020**, *368* (6496), 1274−1278.
(36) Feldman, J.; Bals, J.; Altomare, C. G.; St Denis, K.; Lam, E. C.; Hauser, B. M.; Ronsard, L.; Sangesland, M.; Moreno, T. B.; Okonkwo, V.; Hartojo, N.; Balazs, A. B.; Bajic, G.; Lingwood, D.; Schmidt, A. G. Naive human B cells engage the receptor binding domain of SARS-CoV-2, variants of concern, and related sarbecoviruses. *Sci. Immunol.* **2021**, *6* (66), No. eabl5842, DOI: 10.1126/sciimmunol.abl5842.
(37) Pinto, D.; Park, Y. J.; Beltramello, M.; Walls, A. C.; Tortorici, M. A.; Bianchi, S.; Jaconi, S.; Culap, K.; Zatta, F.; De Marco, A.; Peter, A.; Guarino, B.; Spreafico, R.; Cameroni, E.; Case, J. B.; Chen, R. E.; Havenar-Daughton, C.; Snell, G.; Telenti, A.; Virgin, H. W.; Lanzavecchia, A.; Diamond, M. S.; Fink, K.; Veesler, D.; Corti, D. Cross-neutralization of SARS-CoV-2 by a human monoclonal SARS-CoV antibody. *Nature* **2020**, *583* (7815), 290−295.
(38) Yuan, M.; Wu, N. C.; Zhu, X.; Lee, C. D.; So, R. T. Y.; Lv, H.; Mok, C. K. P.; Wilson, I. A. A highly conserved cryptic epitope in the receptor binding domains of SARS-CoV-2 and SARS-CoV. *Science* **2020**, *368* (6491), 630−633.
(39) Hauser, B. M.; Feldman, J.; Sangesland, M.; Ronsard, L.; St Denis, K. J.; Sheehan, M. L.; Cao, Y.; Boucau, J.; Windsor, I. W.; Cheng, A. H.; Vu, M. L.; Cardoso, M. R.; Kannegieter, T.; Balazs, A. B.; Lingwood, D.; Garcia-Beltran, W. F.; Schmidt, A. G. Cross-reactive SARS-CoV-2 epitope targeted across donors informs immunogen design. *Cell Rep. Med.* **2022**, *3* (12), No. 100834, DOI: 10.1016/j.xcrm.2022.100834.
(40) Hauser, B. M.; Sangesland, M.; Lam, E. C.; Feldman, J.; Balazs, A. B.; Lingwood, D.; Schmidt, A. G. Humoral responses to the SARS-CoV-2 spike and receptor binding domain in context of pre-existing immunity confer broad sarbecovirus neutralization. *Front. Immunol.* **2022**, *13*, No. 902260.
(41) Cameroni, E.; Bowen, J. E.; Rosen, L. E.; Saliba, C.; Zepeda, S. K.; Culap, K.; Pinto, D.; VanBlargan, L. A.; De Marco, A.; di Iulio, J.; Zatta, F.; Kaiser, H.; Noack, J.; Farhat, N.; Czudnochowski, N.; Havenar-Daughton, C.; Sprouse, K. R.; Dillen, J. R.; Powell, A. E.; Chen, A.; Maher, C.; Yin, L.; Sun, D.; Soriaga, L.; Bassi, J.; Silacci-Fregni, C.; Gustafsson, C.; Franko, N. M.; Logue, J.; Iqbal, N. T.; Mazzitelli, I.; Geffner, J.; Grifantini, R.; Chu, H.; Gori, A.; Riva, A.; Giannini, O.; Ceschi, A.; Ferrari, P.; Cippa, P. E.; Franzetti-Pellanda, A.; Garzoni, C.; Halfmann, P. J.; Kawaoka, Y.; Hebner, C.; Purcell, L. A.; Piccoli, L.; Pizzuto, M. S.; Walls, A. C.; Diamond, M. S.; Telenti, A.; Virgin, H. W.; Lanzavecchia, A.; Snell, G.; Veesler, D.; Corti, D. Broadly neutralizing antibodies overcome SARS-CoV-2 Omicron antigenic shift. *Nature* **2022**, *602* (7898), 664−670.
(42) Tortorici, M. A.; Czudnochowski, N.; Starr, T. N.; Marzi, R.; Walls, A. C.; Zatta, F.; Bowen, J. E.; Jaconi, S.; Di Iulio, J.; Wang, Z.; De Marco, A.; Zepeda, S. K.; Pinto, D.; Liu, Z.; Beltramello, M.; Bartha, I.; Housley, M. P.; Lempp, F. A.; Rosen, L. E.; Dellota, E., Jr.; Kaiser, H.; Montiel-Ruiz, M.; Zhou, J.; Addetia, A.; Guarino, B.; Culap, K.; Sprugasci, N.; Saliba, C.; Vetti, E.; Giacchetto-Sasselli, I.; Fregni, C. S.; Abdelnabi, R.; Foo, S. C.; Havenar-Daughton, C.; Schmid, M. A.; Benigni, F.; Cameroni, E.; Neyts, J.; Telenti, A.; Virgin, H. W.; Whelan, S. P. J.; Snell, G.; Bloom, J. D.; Corti, D.; Veesler, D.; Pizzuto, M. S. Broad sarbecovirus neutralization by a human monoclonal antibody. *Nature* **2021**, *597* (7874), 103−108.
(43) Kanekiyo, M.; Joyce, M. G.; Gillespie, R. A.; Gallagher, J. R.; Andrews, S. F.; Yassine, H. M.; Wheatley, A. K.; Fisher, B. E.; Ambrozak, D. R.; Creanga, A.; Leung, K.; Yang, E. S.; Boyoglu-Barnum, S.; Georgiev, I. S.; Tsybovsky, Y.; Prabhakaran, M. S.; Andersen, H.; Kong, W. P.; Baxa, U.; Zephir, K. L.; Ledgerwood, J. E.; Koup, R. A.; Kwong, P. D.; Harris, A. K.; McDermott, A. B.; Mascola, J. R.; Graham, B. S. Mosaic nanoparticle display of diverse influenza virus hemagglutinins elicits broad B cell responses. *Nat. Immunol.* **2019**, *20* (3), 362−372.
(44) Wamhoff, E. C.; Ronsard, L.; Feldman, J.; Hauser, B. M.; Knappe, G. A.; Romanov, A.; Lam, E.; St Denis, K.; Balazs, A. B.; Schmidt, A.; Lingwood, D.; Bathe, M. Enhancing antibody responses by multivalent antigen display on thymus-independent DNA origami scaffolds *bioRxiv* 2022.
(45) Fan, C.; Cohen, A. A.; Park, M.; Hung, A. F.; Keeffe, J. R.; Gnanapragasam, P. N. P.; Lee, Y. E.; Gao, H.; Kakutani, L. M.; Wu, Z.; Kleanthous, H.; Malecek, K. E.; Williams, J. C.; Bjorkman, P. J. Neutralizing monoclonal antibodies elicited by mosaic RBD nanoparticles bind conserved sarbecovirus epitopes. *Immunity* **2022**, *55*, 2419−2435.e10, DOI: 10.1016/j.immuni.2022.10.019.
(46) Caradonna, T. M.; Ronsard, L.; Yousif, A. S.; Windsor, I. W.; Hecht, R.; Bracamonte-Moreno, T.; Roffler, A. A.; Maron, M. J.; Maurer, D. P.; Feldman, J.; Marchiori, E.; Barnes, R. M.; Rohrer, D.; Lonberg, N.; Oguin, T. H., 3rd; Sempowski, G. D.; Kepler, T. B.; Kuraoka, M.; Lingwood, D.; Schmidt, A. G. An epitope-enriched immunogen expands responses to a conserved viral site. *Cell Rep.* **2022**, *41* (6), No. 111628.
(47) Sangesland, M.; Ronsard, L.; Kazer, S. W.; Bals, J.; Boyoglu-Barnum, S.; Yousif, A. S.; Barnes, R.; Feldman, J.; Quirindongo-Crespo, M.; McTamney, P. M.; Rohrer, D.; Lonberg, N.; Chackerian, B.; Graham, B. S.; Kanekiyo, M.; Shalek, A. K.; Lingwood, D. Germline-Encoded Affinity for Cognate Antigen Enables Vaccine Amplification of a Human Broadly Neutralizing Response against Influenza Virus. *Immunity* **2019**, *51* (4), 735−749.e8, DOI: 10.1016/j.immuni.2019.09.001.
(48) Garcia-Beltran, W. F.; Lam, E. C.; Astudillo, M. G.; Yang, D.; Miller, T. E.; Feldman, J.; Hauser, B. M.; Caradonna, T. M.; Clayton, K. L.; Nitido, A. D.; Murali, M. R.; Alter, G.; Charles, R. C.; Dighe, A.; Branda, J. A.; Lennerz, J. K.; Lingwood, D.; Schmidt, A. G.; Iafrate, A. J.; Balazs, A. B. COVID-19 neutralizing antibodies predict disease severity and survival. *Cell* **2020**, *184*, 476−488.e11, DOI: 10.1016/j.cell.2020.12.015.
(49) Garcia-Beltran, W. F.; Lam, E. C.; Astudillo, M. G.; Yang, D.; Miller, T. E.; Feldman, J.; Hauser, B. M.; Caradonna, T. M.; Clayton, K. L.; Nitido, A. D.; Murali, M. R.; Alter, G.; Charles, R. C.; Dighe, A.; Branda, J. A.; Lennerz, J. K.; Lingwood, D.; Schmidt, A. G.; Iafrate, A. J.; Balazs, A. B. COVID-19-neutralizing antibodies predict disease severity and survival. *Cell* **2021**, *184* (2), 476−488 e11.
(50) Moore, M. J.; Dorfman, T.; Li, W.; Wong, S. K.; Li, Y.; Kuhn, J. H.; Coderre, J.; Vasilieva, N.; Han, Z.; Greenough, T. C.; Farzan, M.; Choe, H. Retroviruses pseudotyped with the severe acute respiratory syndrome coronavirus spike protein efficiently infect cells expressing angiotensin-converting enzyme 2. *J. Virol.* **2004**, *78* (19), 10628−10635.
(51) Siebring-van Olst, E.; Vermeulen, C.; de Menezes, R. X.; Howell, M.; Smit, E. F.; van Beusechem, V. W. Affordable luciferase reporter assay for cell-based high-throughput screening. *J. Biomol. Screen* **2013**, *18* (4), 453−461.